J. Membrane Biol. 178, 127–135 (2000)
DOI: 10.1007/s002320010020

The Journal of
Membrane
Biology

Expression and Molecular Characterization of Rat Renal D-Mannose Transport in *Xenopus* Oocytes

T. Blasco[1*], J.J. Aramayona[2*], A.I. Alcalde[2], N. Halaihel[1], M. Sarasa[3], V. Sorribas[1]

[1]Departments of Toxicology, [2]Pharmacology and Physiology, and [3]Anatomy and Embryology, University of Zaragoza, Miguel Servet 177, E-50.013 Zaragoza, Spain

Received: 29 February 2000/Revised: 25 August 2000

Abstract. Renal reabsorption appears to play a major role in D-mannose homeostasis. Here we show that in rat kidney, the transport of D-mannose by brush border membrane vesicles from tubular epithelial cells involves an uphill and rheogenic Na-dependent system, which is fully inhibited by D-mannose itself, incompletely inhibited by D-glucose, D-fructose, phloridzin, and phloretin, and noninhibited by L-mannose or disaccharides. In addition, this system exhibits both low capacity (112.9 ± 15.6 pmol/mg/second) and high affinity (0.18 ± 0.04 mM), with a 2:1 stoichiometry for the Na:D-mannose interaction, and low affinity for sodium (16.6 ± 3.67 mM).

We also show expression of D-mannose transport by *Xenopus laevis* oocytes injected with rat renal polyA$^+$ RNA. Kinetic analysis of the expressed transport was performed after RNA enrichment by fractionation through a sucrose density gradient and was shown to be identical to that measured in membrane vesicles. The RNA species encoding the expressed transport has a small mean size, 1 kb approximately, and shows no homology with the SGLT family of Na-dependent D-glucose transporters, as shown by low stringent RT-PCR and northern analysis. The expressed transport is specific for D-mannose, since in spite of a significant inhibition by D-glucose and D-fructose, neither of these two substrates was transported above the level of the water-injected oocytes.

Key words: Mannose transport — Renal reabsorption — Oocyte expression — *Xenopus laevis* — Membrane vesicles — Rat

Correspondence to: V. Sorribas

* T.B. and J.J.A. contributed equally to the present work.

Introduction

D-Mannose is a hexose mainly used as key component for protein glycosilation in mammal cells that confers high affinity in ligand-receptor interactions [e.g., 1, 10, 21]. All mammal cells can synthesize mannose from glucose and fructose; nevertheless they also contain specific membrane transport systems for the uptake of mannose from the blood [17]. In spite of low mannose plasma concentration (50–70 μM), the affinity of the corresponding transport systems is in a similar range [17, 18, 27], and therefore a continuous supply of the sugar to the cells seems to be guaranteed.

Much of the information published during recent years has suggested an important role by the kidney in controlling D-mannose homeostasis. For instance, in vivo studies have clearly shown that after free filtration through the glomerulus, most of the mannose is readily reabsorbed [18, 19, 22, 32]. In addition, a general consistency of both in vivo [18, 19, 22, 32] and in vitro [15, 19, 23, 27] studies has led to detailed functional and kinetic knowledge, whose main characteristics are indicated below.

D-Mannose is actively reabsorbed through a specific transport system, which is also shared or inhibited by D-fructose [2, 15] and 1,5-anhydro-D-glucitol [18, 19, 22, 32]. D-Glucose also inhibits D-mannose reabsorption, but this has been proposed to be an indirect effect, as a consequence of competition and dissipation of the Na^+ electrochemical gradient [15]. Detailed kinetic knowledge of D-mannose transport has also been obtained by using brush border membrane vesicles (BBMV) from both dog kidney [15, 23] and the tubular epithelial cells of winter flounder [19], as well as in vitro studies with several permanent cell lines [17]. In summary, D-mannose seems to be reabsorbed through a unique rheogenic and uphill Na-coupled transport system, with 1:1

Na:D-mannose stoichiometry that is inhibited by the Na/D-glucose cotransport inhibitor, phloridzin. The D-mannose transport system has high affinity and low capacity, with Michaelian values ranging from K_m 127 μM and V_{max} 3 pmol/mg/sec in winter flounder [19] to K_m 70 μM and V_{max} 60 pmol/mg/sec in dog BBMV [15, 23], and K_m 80 μM and V_{max} 1.4 pmol/mg/sec in MDCK cells [17].

In spite of the extensive functional and kinetic analysis to date, several questions remain unclear, which could be answered with different, molecular tools. For instance, it is difficult to explain, at least in kinetic terms, the fact that D-glucose and α-methyl-D-glucoside partially inhibit D-mannose transport, but D-mannose is unable to decrease D-glucose reabsorption [15, 32]. The same can be said about D-fructose, which is able to inhibit D-mannose reabsorption but does not affect D-glucose renal transport [15, 18, 32]. Finally, the role of the Na/D-glucose cotransport inhibitor, phloridzin, is also puzzling. This sugar derivative readily inhibits Na/D-mannose cotransport, although with at least ten times less affinity than the Na/D-glucose, and through a different, noncompetitive mechanism [15, 23].

The aim of the present work has been to contribute to the knowledge of D-mannose renal reabsorption by using rat kidney BBMV and additional molecular approaches. First, we have shown that rat BBMV behave similarly to dog membranes with respect to D-mannose transport. Second, we have been able to express the same rat renal high affinity D-mannose transport in *Xenopus laevis* oocytes by injecting polyA$^+$ RNA. The expressed transport has been kinetically characterized and shown to be directly inhibited by, at least, D-glucose, phloridzin, phloretin, and D-fructose. Finally, sucrose density gradient mRNA fractionation has shown that a small RNA of about 1 kb encodes the expressed transporter, therefore different from the SGLT-1, SGLT-2, and the GLUT transporters. This study opens up the possibility for directly cloning this membrane protein by functional expression and screening in a cDNA library.

Materials and Methods

Brush Border Membrane Preparation and Transport Assays

Brush border membrane vesicles were prepared from the whole kidney cortex of 2- to 3-month-old Wistar rats (Harlan Ibérica S.A., Barcelona, Spain), as described [16, 26]. In short, the whole kidney cortex was cut into thin slices at 4°C, and homogenized with a Disperser DIAX 600 (Heidolph, Kelheim, Germany) in a buffer consisting of (mM): 300 DL-mannitol, 5 EGTA, 0.5 phenylmethylsulfonyl fluoride, and 16 Hepes (pH 7.5 with Tris). The BBMs were purified from this homogenate by Mg^{2+} precipitation and differential centrifugation. The final pellet was dissolved in a buffer of 300 mM mannitol, and 16 mM Hepes-Tris, pH 7.5. Purity of the BBM preparations was assayed by measuring enzyme activities as published [8] and measurement of the Na-dependent D-glucose overshoot.

Trasport measurements were performed on freshly isolated BBMV at 25°C through the uptake of various concentrations of D-mannose plus D-[2,6-^{3}H] mannose (40 Ci/mmol, American Radiolabeled Chemicals, ARC, St. Louis, MO) as a radio tracer (at least 4 μCi/ml of uptake medium) and an inwardly directed sodium gradient (100 mM), followed by rapid filtration. Osmolarity of the incubation medium was kept constant by using mannitol. In control experiments we found no differences between mannitol or sorbitol osmotic agents on D-mannose uptake. For transport assays in the absence of Na, this metal was equimolarly substituted by choline chloride, KCl or KSCN.

Isolation of RNA, mRNA, and Sucrose Gradient Fractionation

Total RNA was isolated from kidney cortex as explained [2], according to the guanidium thiocyanate-phenol acid-chloroform method [5]. PolyA$^+$ RNA was purified from total RNA using two different methods: hybridization to oligo dT-biotin plus recovery by streptavidin-conjugated magnetic particles (mRNA Isolation Kit, Roche Molecular Biochemicals, Mannheim, Germany) and binding to oligo dT-cellulose in spin columns (PolyA Pure kit, Ambion, Austin, TX). Sucrose gradient fractionation was performed as described [24] using 100 μg of highly pure mRNA. RNA was denatured, electrophoresed in a formaldehyde agarose gel, transferred onto Hybond N$^+$ nylon membranes (Amersham Pharmacia Biotech, Buckinghamshire, UK) and UV cross-linked (UVC 500, Hoeffer, San Francisco, CA) for further analysis. Gels and membrane blots were analyzed with a Gel Doc 1000 Video Gel Documentation System (Bio-Rad Laboratories, Hercules, CA).

Preparation of Oocytes and Measurement of D-Mannose Uptake

All methods relating to the preparation, injection, and incubation of oocytes (stage V/VI) were followed by precisely observing the protocols described earlier [11, 31]. mRNA (5–50 ng/50 nl/oocyte) was microinjected using a Nanoliter Injector (World Precision Instruments, WPI, Hertfordshire, UK). Na-dependent (100 mM) and Na-independent (sodium replacement by choline) uptake of D-mannose by oocytes was studied at 25°C, using D-[2,6-^{3}H] mannose (at least 40 μCi/ml; ARC) as a substrate.

RT-PCR

Two-step reverse transcriptase followed by polymerase chain reaction amplification was performed on the fractionated or total mRNA, using MMLV reverse transcriptase (First-Strand cDNA Synthesis Kit) and Taq DNA polymerase (both from Amersham Pharmacia Biotech, Uppsala, Sweden) in a PTC-100 thermal cycler (MJ Research, Watertown, MA) following the instructions supplied with the kit. Primers were designed to amplify a 1296 bp fragment of the rat type 1 Na/D-glucose cotransporter (SGLT1) cDNA using Oligo 6.1 software: primer 131U18, GAC AGT AGC ACC TTG AGC and primer 1410L17, CAG CAC GAG GAT GAA CA.

Northern Analysis

Blots from the mRNA sucrose gradient fractionation were hybridized using the PCR products described in the previous paragraph as probes.

The DNA products were labeled with [α-^{32}P]-dATP (3,000 Ci/mmol) by random priming (RadPrime DNA Labeling System; Gibco-BRL-Life Technology, Grand Island, NY), and hybridization was carried out at low stringency (30% formamide) as described [9]. Signals were analyzed with the Gel Doc 1000 (Bio-Rad) after exposure to Hyperfilm MP X-ray films (Amersham Pharmacia Biotech, Buckinghamshire, UK).

Data Analysis

All results are expressed as the mean ± SEM; means were calculated from triplicates in vesicle uptake values (filters) or from 8–10 oocyte values. Results obtained from individual membrane vesicle or oocyte preparations are shown throughout the paper. Qualitatively identical data have been obtained in at least three different preparations. When necessary, means are compared by a one-way analysis of variance (ANOVA) using a Dunnett post test to compare pairs of group means.

Kinetic analysis of sodium or D-mannose saturating kinetics was performed by nonlinear regression using GraphPad Prism 2.0 (GraphPad, San Diego, CA) on an iMac microcomputer. Curves relating to the saturation of D-mannose (DM) transport in both BBMV and oocytes were obtained as published [24, 25] using an equation containing a saturable component (Michaelis-Menten) plus a diffusion uptake term (nonsaturable): $V = (V_{max}[DM]/(K_{DM} + [DM])) + K_D[DM]$. In these experiments, fit convergence was achieved by minimizing the sum of the squares of relative distances of points from the curve. Michaelian analysis of the mRNA specific expressed transport was performed after subtracting the D-mannose transport of water injected oocytes from the total transport of mRNA injected. In this case, the equation contained a saturable component only. Na-independent D-mannose transport was also fitted into a single diffusion component equation (linear uptake). Curves relating to the sodium saturation of the Na-dependent D-mannose uptake were obtained by using a generalized Hill equation: $V = V_{max}[Na]^n/(K^n_{Na} + [Na]^n)$. In this case, fit convergence was achieved by minimizing the sum of the squares of the actual distance of points from the curve. In both equations, V is D-mannose influx in pmol/mg/sec for membrane vesicle experiments, or pmol/oocyte/min; V_{max} is the maximal D-mannose influx rate; [DM] and [Na] are the external D-mannose or sodium concentrations in mM; K_{DM} and K^n_{Na} are the apparent affinity constants for D-mannose and sodium, respectively, in mM; n, the Hill coefficient or slope, is an estimate of the number of reactive Na-binding sites; and K_D is a diffusion constant, in nl/mg/second (for membrane vesicles) or nl/oocyte/min.

Results

Transport of D-Mannose in Brush Border Membrane Vesicles from Rat Kidney Cortex

These experiments were performed prior to the expression in oocytes in order to check for similarity with previous works (*see* Introduction). The time-course experiments (Fig. 1*A*) using 50 μM D-mannose in the absence of sodium were linear in time and independent of the salt used (choline chloride, KCl, or KSCN). This uptake was activated by sodium (NaCl), showing a small but significant overshoot (i.e., uphill transport) that was further stimulated by the presence of a thiocyanate anion (NaSCN), therefore suggesting the existence of a Na-coupled and, most likely, rheogenic/electrogenic D-mannose renal transport. These results are similar to those previously described in winter flounder [19] and dog [15] renal BBMV. In addition, we found no differences between the D-mannose transport characteristics in superficial *vs.* juxtamedullar renal cortex membrane vesicles.

D-Mannose saturating kinetics were performed at 5 sec (initial velocity, *data not shown*). They are depicted in Fig. 1*B* as the total transport in the presence (NaCl) and absence (choline-Cl) of Na^+ and as the Na-dependent component after subtracting the Na-independent uptake from the total (Na^+ present) values. Michaelian constants calculated by nonlinear regression are shown in the Table. Similar to previous literature, rat kidney shows the existence of an accumulating Na-coupled D-mannose transport of high affinity and low capacity that correlates with the low D-mannose plasma concentration. In our vesicle preparations, D-mannose exhibited a high diffusion rate when compared to D-glucose kinetics (K_d for D-glucose 5–10 nl/mg/second). Moreover, Na-saturating kinetics (Fig. 1*C* and Table) performed with 0.1 mM D-mannose shows typical Na/substrate interaction with 2:1 stoichiometry (Hill coefficient >2) and high K_{Na}.

Finally, the pattern of D-mannose transport inhibition is also similar to previous reports. Figure 1*D* shows inhibiton of the Na-dependent component of the D-mannose (50 μM) transport by several substrates. Na-dependent D-mannose transport by BBMV was completely abolished by 50 mM D-mannose (uptake was not statistically different from Na-independent transport), and partially inhibited by 50 mM D-glucose (53.6%), 0.5 mM phloridzin (80.2%; an inhibitor of Na/coupled D-glucose transport, mediated by the SGLT transporters), 0.1 mM phloretin (59.8%; an inhibitor of Na-independent D-glucose transport, mediated by the GLUT transporters), and 50 mM D-fructose (62.2%). L-Mannose, L-leucine, or disaccharides as maltose and lactose (all at 50 mM) did not affect D-mannose transport.

Expression of Rat Renal D-Mannose Transport in *Xenopus laevis* Oocytes

The expression of D-mannose transport in *Xenopus* oocytes was of low intensity but similar to other protein expressions [13, 24]; 0.1 mM D-Mannose uptake was measured at 25°C and 1 hr of incubation in the presence and absence of 100 mM Na^+. Injection of 25 ng/oocyte of rat kidney cortex mRNA elicited a linear increase of Na-dependent D-mannose transport with incubation days in a Barth's solution. Figure 2*A* shows Na-dependent uptake in water and RNA-injected oocytes. The expressed transport in the presence of Na^+ was significantly different from the water-injected oocytes after 6 days of

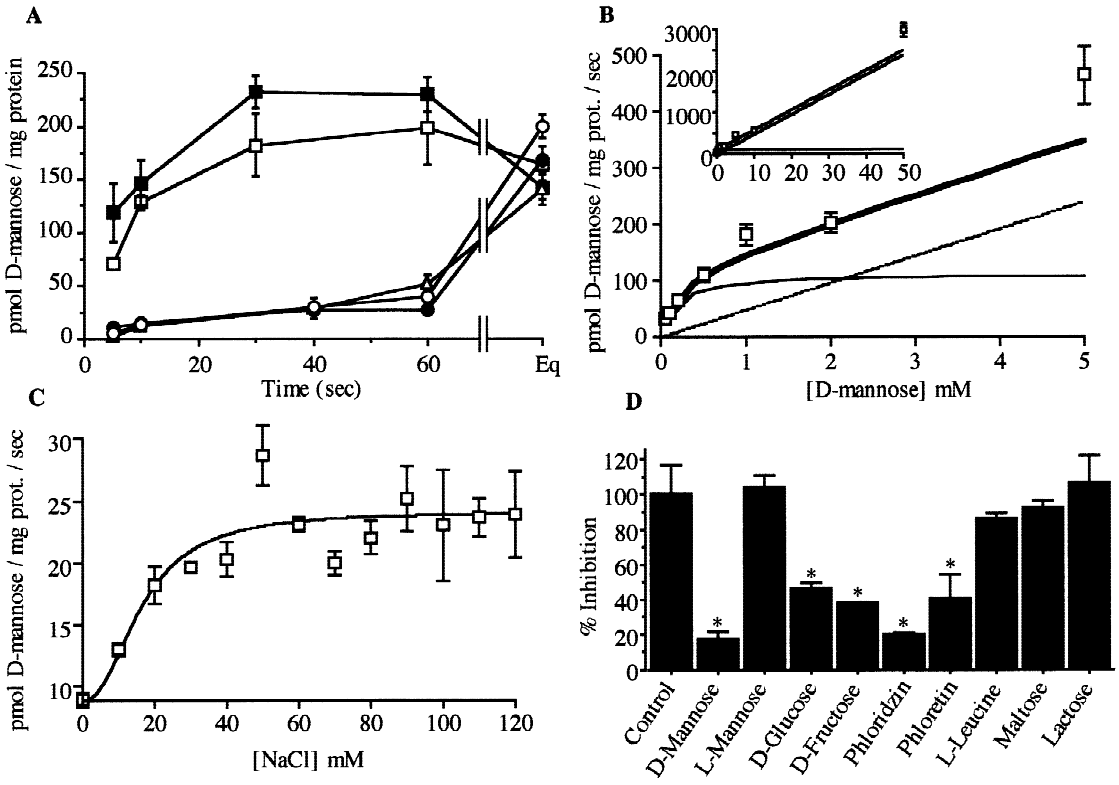

Fig. 1. Transport of D-mannose by brush border membrane vesicles from rat kidney. Open squares, uptake in the presence of NaCl; black squares, uptake in NaSCN; open circles, KCl; black circles, KSCN; triangles, choline chloride. (*A*) Time course of D-mannose uptake showing Na-activation. Uptake in the absence of Na is linear over time. (*B*) D-mannose saturating kinetics in the presence of 100 mM NaCl, showing theoretical decomposition of total uptake (bold line) into the diffusion component (dashed line) and the saturable component (normal line). Inset, the complete figure showing the full range of substrate concentrations used. (*C*) Sodium chloride saturating kinetics of D-mannose transport showing a typical Na:substrate interaction with 2:1 stoichiometry. (*D*) Pattern of net Na-dependent D-mannose (0.05 mM) transport inhibition with 50 mM D-mannose, 50 mM L-mannose, 50 mM D-glucose, 50 mM D-fructose, 0.5 mM phloridzin (Phloz) and 0.1 mM phloretin (Phlot), 50 mM L-leucine, 50 mM maltose, and 50 mM lactose.

expression and maximal after 8 days. The expressed transport was shown to be completely Na-dependent, since there was no expression in the absence of sodium (e.g., Fig. 2*D*). In addition, water-injected oocytes also exhibited a Na-stimulated component of D-mannose transport. The dose-response relationship was measured after 6 days of injecting different amounts of renal mRNA (Fig. 2*B*). Transport expression was already saturated at 25 ng/oocyte under the same experimental conditions of Fig. 2*A*.

A time-course analysis performed in order to find out the initial velocity limits of the D-mannose transport showed that the uptake was linear, at least, for 4 hr of incubation with hot D-mannose and already significantly different from water-injected oocytes after 30 min (Fig. 2*C*). Therefore, the parameters chosen for the ensuing experiments were 8 days of expression, 25 ng RNA per oocyte, and 1 hr incubation time, even if some of the mannose was metabolized inside the oocyte (the concentration of the sugar reached inside the cell is very low, 1–5 μM).

Oocytes were also injected with RNA isolated from superficial (SC) or juxtamedullar (JM) cortex. Surprisingly, in contrast to the vesicle experiments, only SC RNA was able to express D-mannose transport (Fig. 2*D*); as controls, Na-dependent D-glucose and Na-independent L-arginine uptakes are shown. Finally, experiments performed at 25°C or 37°C showed that the increase in temperature proportionally stimulated both transport components, those intrinsic to the oocyte and those expressed by the RNA, and therefore the stimulation percentage remained unaltered (*data not shown*).

Sucrose Gradient Fractionation of Rat Renal mRNA

Two density gradient fractionations were performed in this work, with qualitatively identical results. Figure 3*A* shows an mRNA fractionation agarose gel, with numbered fractions and molecular weights. 25 ng of each RNA fraction were injected into oocytes, and the results

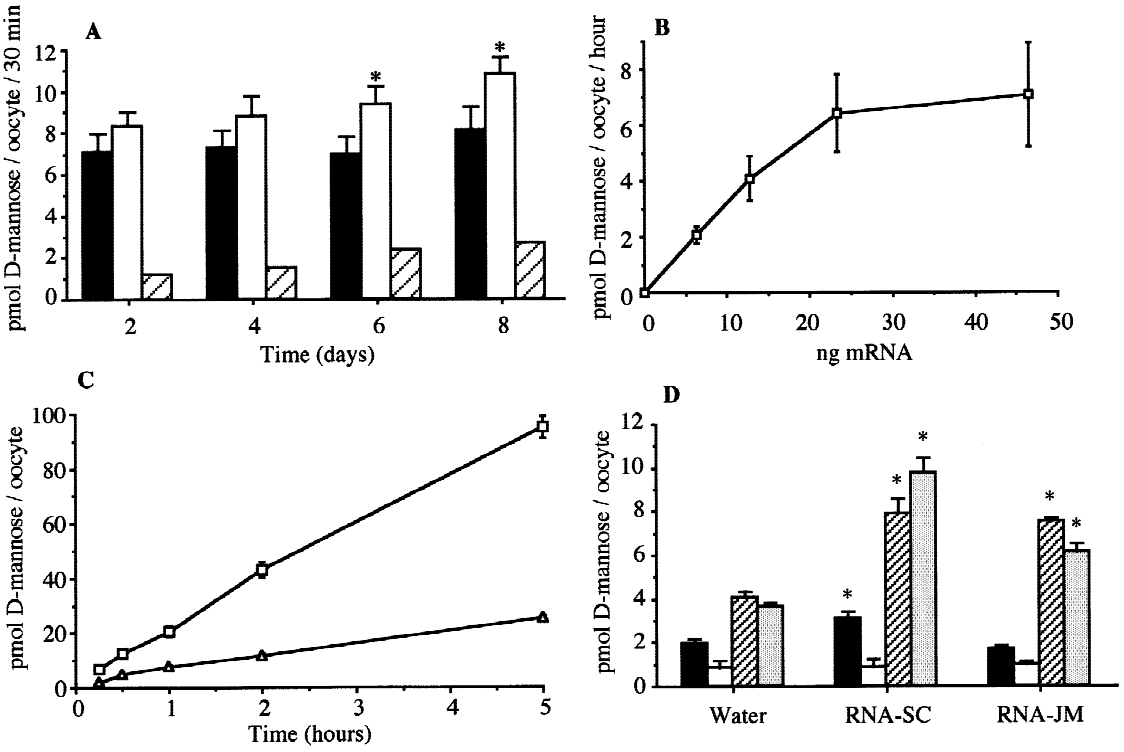

Fig. 2. Expression of D-mannose transport in *Xenopus laevis* oocytes. (*A*) Expression as a function of post-injection days. Black bars, water-injected oocytes; white bars, RNA injected oocytes; lined bars, mRNA specific transport. (*B*) Dose-response of RNA injection on D-mannose transport. Figure only shows mRNA specific mannose uptake. (*C*) Time course of D-mannose uptake in water (triangles) and RNA (squares) injected oocytes. (*D*) Expression of D-mannose transport by RNA from superficial (SC) and from juxtamedullar (JM) cortex. Black bars, D-mannose transport in the presence of 100 mM NaCl. White bars, Na independent D-mannose uptake. Lined bars, D-glucose uptake in the presence of 100 mM NaCl. Dotted bars, Na-independent L--arginine uptake. Asterisks in D are significant differences from the corresponding values of water-injected oocytes.

of the expression are shown in Fig. 3*B*. Fractions 9 to 11, encoding RNAs of only 0.7 to 1.4 kb, elicited expression of D-mannose transport statistically different from the water injected oocytes. More precisely, while nonfractionated mRNA expressed 1.8 times more D-mannose transport than water injected oocytes, RNAs from these three fractions expressed almost 3 times more than the basal level. Again, no expression of D-mannose transport by any fraction in the absence of Na was observed. The surprising size of the encoding fractions was also checked by RT-PCR and northern blot analysis (see below).

Kinetic Analysis of Expressed Transport

Fractionated RNA was used to kinetically characterize the expressed transport (Fig. 4*A* and *B*). Experimental results were fit into saturating equations as explained in Materials and Methods and are summarized in the Table. mRNA-specific D-mannose uptake was kinetically similar to the transport measured in brush border membrane vesicles. D-Mannose saturating kinetics gave an affinity constant of 0.08 mM, while sodium saturating kinetics showed the predicted 2:1 Na:D-mannose stoichiometry and a K_{Na} of 29.9 mM (capacity of the transport system is mainly a result of the oocyte batch expression ability and the amount of injected RNA).

Specificity of D-Mannose Transport

The expressed transport from fractionated RNA was also used to study the specificity of the D-mannose transport. Figure 5*A* shows the inhibition of 0.1 mM of D-mannose transport by several substrates. As expected, while D-mannose transport was only completely abolished by D-mannose itself, partial inhibition was also observed in the presence of D-glucose, D-fructose, phloridzin, and phloretin. Interestingly, the two last inhibitors did not affect the intrinsic D-mannose transport system of the oocyte.

It has been proposed that D-glucose inhibition in BBMV from dog kidney is noncompetitive and caused by the dissipation of the Na electrochemical gradient [15]. In addition, a less-analyzed inhibition by D-fructose has led to the conclusion that D-mannose and D-fructose share the same reabsorption route [32]. To clarify these two inhibitions, oocytes injected with the

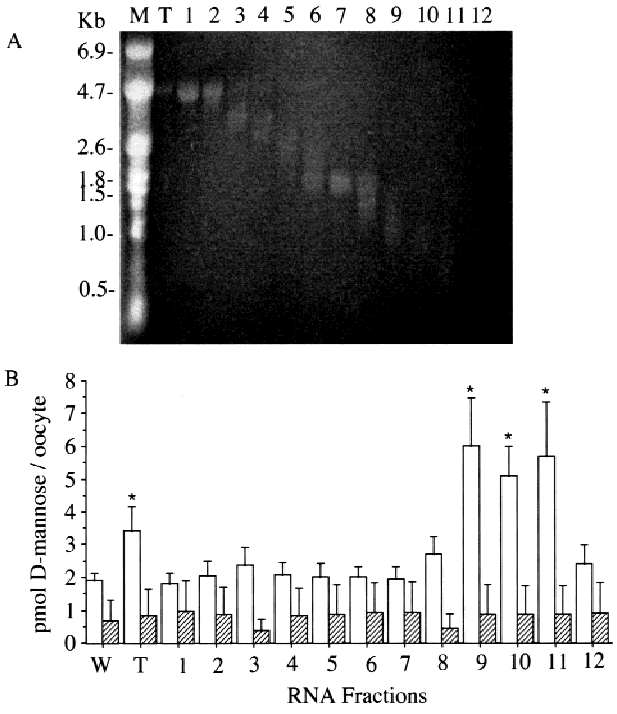

Fig. 3. Sucrose gradient fractionation of renal cortex mRNA. (*A*) Formaldehyde agarose gel showing renal RNA size fractionation after density gradient centrifugation: M, RNA molecular marker, sizes indicated at the left; T, total (nonfractionated) mRNA; 1–12, RNA fractions, from high to low molecular weights; Kb, kilobases. (*B*) Uptake of D-mannose by oocytes injected with water or the corresponding fractionated RNA, as indicated in *A*. White bars, Na-coupled D-mannose transport; lined bars, Na-independent uptake. W, water injected oocytes. T, total mRNA.

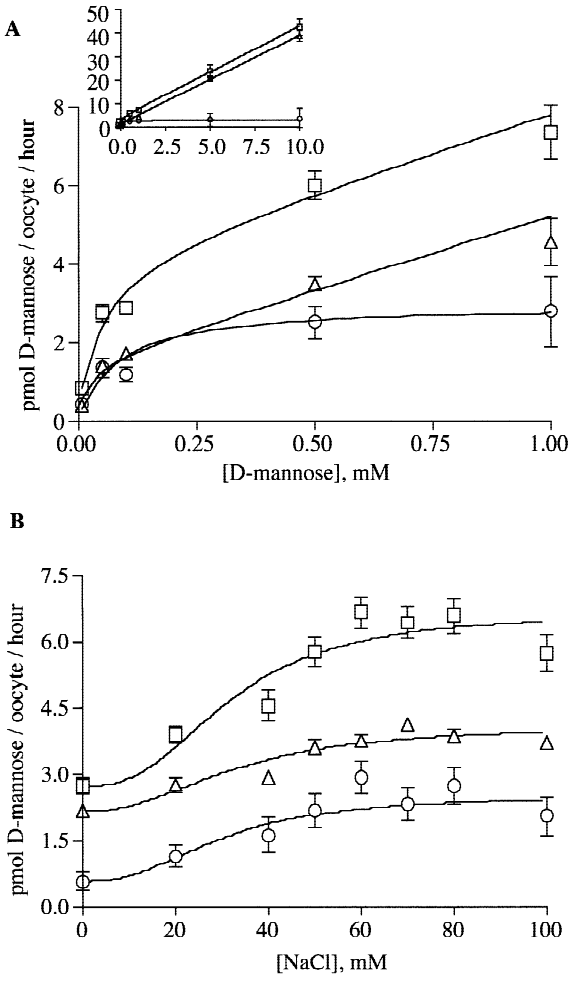

Fig. 4. Kinetic analysis of D-mannose transport in *Xenopus* oocytes. Oocytes were injected with fractionated RNA (fractions 9–11 of Fig. 3). mRNA specific values were obtained by subtracting the means of water-injected oocytes from the means of RNA-injected oocytes. Symbols are: squares, RNA-injected; triangles, water-injected; circles, net expressed transport. Michaelis values are shown in the Table. Inset in *A* corresponds to the full range of D-mannose concentrations used.

RNA fraction encoding the transcript(s) responsible for the D-mannose transport were checked for ^{14}C-D-glucose and ^{14}C-D-fructose transport. As can be observed in Fig. 5*B*, we did not find expression of transport of either substrate, therefore suggesting another kind of noncompetitive inhibition.

Structural Relationships

Because of the inhibitions caused by D-glucose and D-fructose, we also decided to check for homology between the carrier responsible for D-mannose transport and the Na/D-glucose cotransporter, more precisely the rat SGLT1 [7]. Two experiments were performed in order to achieve this objective. First, as explained in Materials and Methods, we amplified a conserved open reading frame from the rat SGLT1 cDNA by RT-PCR from the total rat kidney mRNA and from the mRNA fraction corresponding to the size of the SGLT1 mRNA (fraction 5 in Fig. 3*A*). However, we were unable to amplify anything from the fractions expressing D-mannose transport (Fig. 6*A*). Second, the 1296 bp SGLT1 product was used as a radioactive probe to be hybridized at low stringency with the membrane blot from the mRNA fractionation agarose gel shown in Fig. 3*A*. This second test was used, because the PCR method needs a perfect match at the oligonucleotide 3′-end, independently of the homology of the rest of the primer sequence. Figure 6*B* shows the expected signals in the total and fraction 5 mRNA lanes, but we found no signals in the fractions expressing the D-mannose transport, even at 30% formamide and low stringent (room temperature) post-hybridization washes, therefore suggesting that both proteins ought to be structurally unrelated.

Discussion

In the present work, we have tried to answer some questions posed by previous kinetic studies on D-mannose

Table. Kinetic analysis of D-mannose renal transport in brush border membrane vesicles and *Xenopus laevis* oocytes

BBMV	V_{max}	K_m	K_d	
Mannose kinetics	pmol/mg/sec	mM	nl/mg/sec	*df, r*
NaCl	112.90 ± 15.64	0.18 ± 0.04	47.89 ± 3.31	34, 0.9487
Choline	—	—	68.67 ± 8.32	36, 0.9291
Sodium kinetics			*n*	*df, r*
	15.32 ± 1.36	16.61 ± 3.67	2.23 ± 1.09	60, 0.3521
OOCYTES				
	V_{max}	K_m	K_d	
Mannose kinetics	pmol/oocyte/hour	mM	nl/oocyte/hour	*df, r*
H_2O NaCl	1.60 ± 0.22	0.033 ± 0.008	3.03 ± 0.24	63, 0.9126
RNA NaCl	3.72 ± 0.34	0.040 ± 0.007	3.33 ± 0.25	62, 0.8771
Net NaCl	2.96 ± 0.42	0.080 ± 0.028	—	5, 0.8769
Sodium kinetics			*n*	*df, r*
H_2O	1.96 ± 0.28	33.54 ± 6.19	2.24 ± 0.80	69, 0.6515
RNA	3.91 ± 0.49	32.03 ± 5.18	2.68 ± 0.90	73, 0.5911
Net	1.94 ± 0.45	29.90 ± 9.12	2.46 ± 1.37	5, 0.8064

df, degrees of freedom; *r*, regression coefficient. Constant values are mean ± SEM.

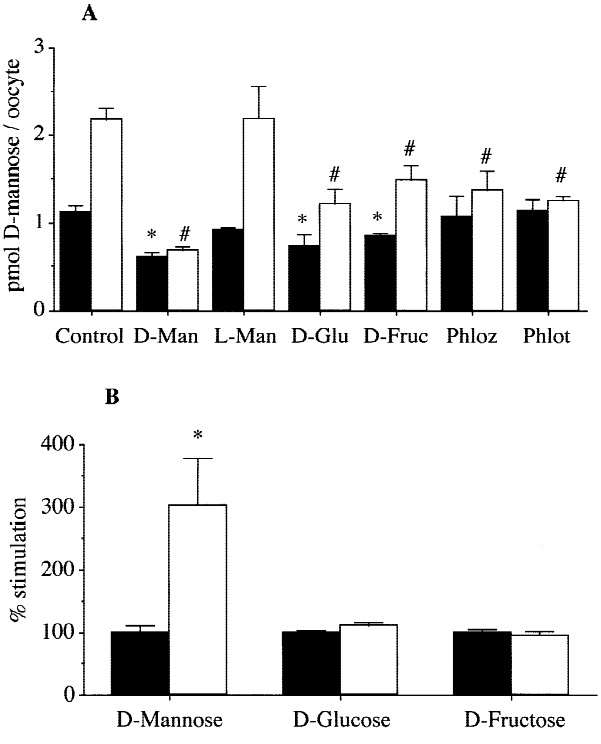

Fig. 5. Inhibition and specificity of expressed transport. Black bars, water-injected oocytes; white bars, RNA-injected oocytes (fractions 9–10 of Fig. 3). (*A*) Inhibition of 0.1 mM D-mannose transport by several substrates at 100 mM (D-mannose, L-mannose, D-glucose, and D-fructose), 1 mM phloridzin, and 0.1 mM phloretin. * and # are significant differences from the corresponding water and RNA control values. (*B*) Expression of D-mannose, D-glucose, and D-fructose transport by the RNA fraction expressing D-mannose transport.

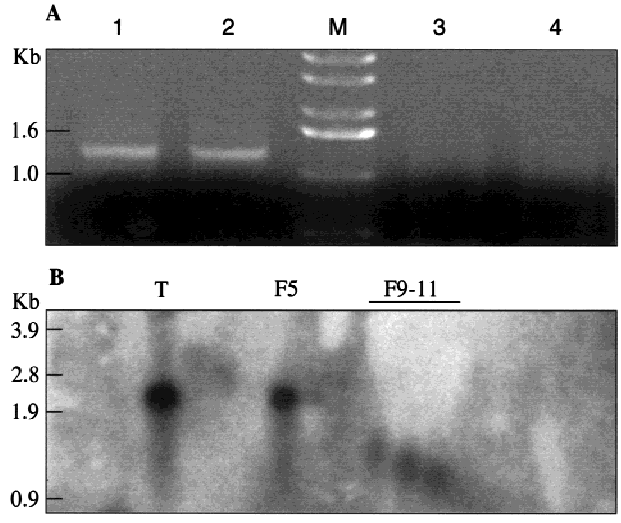

Fig. 6. (*A*) RT-PCR, showing amplification of SGLT1 fragment from total RNA (lane 1) and the RNA fraction corresponding to the size of the cloned rat SGLT1 (2; lane 5 of Fig. 3). Lanes 3 and 4 correspond to two fractions expressing D-mannose transport in oocytes (lanes 9 and 10 of Fig. 3) (*B*) Northern blot from a size-fractionated RNA, showing hybridization signals using the SGLT1 DNA product from *A* as a radioactive probe. No signal was obtained in RNA fractions expressing D-mannose transport, even under the low strigency conditions (*see* background at the right).

renal reabsorption by using the expression of rat kidney mRNA in *Xenopus* oocytes. Those previous works focused on the physiological analysis of mannose renal reabsorption, showing that this hexose is transported in the proximal tubule by a unique Na-coupled transport system of high affinity and low capacity [15, 17–19, 23, 32]. Even so, the system was shown to be inhibited by several substrates such as D-glucose, D-fructose, phloridzin, phloretin, 1,5-anhydro-D-glucitol, etc., and these findings were interpreted, in some cases, as the result of direct competition for a common carrier. Furthermore, the excellent work by the Silverman group [15, 23] almost exhausted all possibilities of kinetic analysis to obtain additional physiological information on D-mannose

renal transport; for instance, in spite of the inhibition by D-glucose, they stated that the transport system was still specific for D-mannose.

Our work has increased this knowledge in several ways. First, we have been able to express exogenous (rat superficial kidney cortex) D-mannose transport in *Xenopus laevis* oocytes, therefore setting up the possibility for direct cloning of the corresponding transporter by functional expression (homology cloning using other transporter sequences seems to be unsuccessful after our results with RT-PCR and northern blotting, shown in Fig. 6). In fact, the pattern of expression, although quantitatively small (only two to three times the intrinsic level using size-fractionated RNA), has been common for most of the expressed membrane proteins, mainly in terms of dose-response and expression-time. Second, we have restricted the molecular size of the responsible mRNA species to approximately 1 kilobase, therefore differentiating this transporter from other previously identified sugar carriers, all of them with larger molecular sizes. And third, we have partially clarified the kind of inhibition by D-glucose and D-fructose on D-mannose transport.

As indicated above, the average size of the RNA species expressing D-mannose transport is very small when compared with the molecular weight of other transporter RNAs, since most of them range between 2 and 4 kb. Some examples are the SGLT [29] and GLUT [28] groups of D-glucose transporters, phosphate [11, 25], sulfate [12], and organic anion/cation transporters [6], amino acid transporters [e.g., 4], etc. The predicted low molecular weight could be, however, partially compensated with very short 5′ and 3′ untranslated regions, therefore leading to a larger (but still uncommonly small) open reading frame. A different possibility is that the characterized RNA does not encode a real transporter rather a modulator of existing transporters. For instance, since the oocyte expressing system exhibits an intrinsic component of Na-coupled D-mannose transport (*see* Table), the RNA species responsible for the expressed transport measured could *simply* be a regulator (stimulator) of the endogenous transport system of the oocyte. This possibility cannot be fully discarded because both transport systems exhibit a similar affinity constant. However, the fact that the affinity constant of the BBMV (0.18 ± 0.04 mM) is closer to the K_m of the expressed transport (0.080 ± 0.028 mM) than to the K_m of the endogenous transport (0.033 ± 0.008 mM) and that the inhibition pattern is also different, in that phloridzin and phloretin do not inhibit the intrinsic transport of the oocyte (*see* Fig. 5*A*), all of these results suggest that the transport that we are expressing corresponds indeed to the rat kidney. Other possibilities, as a modulator modifying only the capacity of the system but not its affinity, cannot be excluded.

Inhibition by D-glucose and D-fructose also provide new insight into mannose transport analysis. Although still consistent with a noncompetitive pattern of inhibition, our results clearly eliminate the theory that Na^+ electrochemical gradient dissipation is responsible for such inhibition, since neither D-glucose nor D-fructose were differentially accumulated into the oocytes injected with the fractionated RNA (*see* Fig. 5*B*). However, because of the interaction existing between these two sugars, an alternative possibility cannot be excluded, which is that the RNA responsible for the expressed D-mannose transport could encode a protein that modifies the activity of endogenous carriers for D-glucose and D-fructose in the oocyte. Two examples illustrate this possibility. The first is the RS1 [30], an almost cytosolic protein that modifies the activity of at least two membrane transporters, the sodium D-glucose cotransporter SGLT1, and the organic cation transporter OCT1 [20, 30]. Both the molecular weight and the mechanistic differences exclude the possibility of an RS1-type protein being involved in D-mannose transport. The second example involves receptor-activity modifying proteins 1 to 3 (RAMP1-3), i.e., cytosolic proteins that, after binding to calcitonin receptorlike receptors (CRLR), change the specificity of these membrane proteins towards, at least, two different neuropeptides, adrenomedullin or the calcitonin gene-related peptide [14]. More possibilities could be suggested, but only cloning of the cDNA responsible for the D-mannose expressed transport will clarify definitively its function, structure, and location in the cell.

With respect to the third main contribution, the inhibition by D-glucose and D-fructose, we have shed light on previous data [15] about D-glucose inhibition of D-mannose in BBMV from dog kidney. Through analysis of inhibition kinetics, the authors concluded that this effect was either noncompetitive or pseudocompetitive [3], therefore a consequence of any, allosteric modifications to the protein with two different binding sites (for D-mannose and D-glucose) on the same carrier, or due to the dissipation of the Na^+ electrochemical gradient. In our work, we have excluded the second possibility, as well as a fully competitive inhibition (competition for a unique binding site), since D-glucose is not transported by the oocytes expressing the fractionated RNA. Therefore the existence of a recognition site for D-glucose different from the D-mannose site seems to be the most likely explanation. The same could be said about D-fructose inhibition, as well as phloridzin and phloretin.

Finally, contradictory information arises with respect to the anatomic localization of the transport we are measuring. While membrane vesicles have shown that uphill D-mannose transport takes place in both the superficial and juxtamedullar renal cortex, only RNA from the SC cortex was able to elicit D-mannose transport over the intrinsic uptake of the oocyte in three independent ex-

periments (quality of the JM RNA was always checked by measuring D-glucose and L-arginine uptakes). One possible explanation is that we are measuring two different proteins, each one more abundant in the SC and JM cortex, but only the SC being able to be expressed in *Xenopus* oocytes.

In conclusion, we have molecularly characterized the D-mannose transport system from rat kidney cortex in *Xenopus* oocytes, showing that it is mediated by a new protein with low molecular weight and susceptible to pseudocompetitive inhibition by other sugars or sugar derivatives.

Our thanks to Prof. F. Alvarado (CNRS, France) and Prof. Moshe Levi (VAMC, Dallas) for their critical comments on the manuscript. This work was supported by the P-45/96 grant from CONSID-Government of Aragón.

References

1. Aderem, A., Underhill, D.M. 1999. Mechanisms of phagocytosis in macrophages. *Annu. Rev. Immunol.* **17:**593–623
2. Alcalde, A.I., Sarasa, M., Raldúa, D., Aramayona, J., Morales, R., Biber, J., Murer, H., Levi, M., Sorribas, V. 1999. Role of thyroid hormone in regulation of renal phosphate transport in young and aged rats. *Endocrinology* **140:**1544–1551
3. Alvarado, F. 1978. Resolution by graphical methods of the equations for allosteric competitive inhibition and activation in michaelian enzyme and transport systems. *J. Physiol.* **74:**633–639
4. Bertrán, J., Testar, X., Zorzano, A., Palacín, M. 1994. A new age for mammalian plasma membrane amino acid transporters. *Cell Physiol. Biochem.* **4:**217–241
5. Chomcyznski, P., Sacchi, N. 1987. Single-step method of RNA isolation by acid guanidium thiocyanate-phenol-chloroform extraction. *Anal. Biochem.* **162:**156–159
6. Koepsell, H. 1998. Organic cation transporters in intestine, kidney, liver, and brain. *Annu. Rev. Physiol.* **60:**243–266
7. Lee, W.S., Kanai, Y., Wells, R.G., Hediger, M.A. 1994. The high affinity Na^+/glucose cotransporter: Reevaluation of function and distribution of expression. *J. Biol. Chem.* **269:**12032–12039
8. Levi, M., Baird, B.M., Wilson, P.W. 1990. Cholesterol modulates rat renal brush border membrane phosphate transport. *J. Clin. Invest.* **85:**231–237
9. Levi, M., Lötscher, J., Sorribas, V., Custer, M., Arar, M., Kaissling, B., Murer, H., Biber, J. 1994. Cellular mechanisms of acute and chronic adaptation of rat renal Pi transporter to alterations in dietary Pi. *Am. J. Physiol.* **267:**F900–F908
10. Liu, Q., Grubb, J.H., Huang, S.S., Sly, W.S., Huang, J.S. 1999. The mannose 6-phosphate/insulin-like growth factor-II receptor is a substrate of type V transforming growth factor-beta receptor. *J. Biol. Chem.* **274:**20002–20010
11. Magagnin, S., Werner, A., Markovich, D., Sorribas, V., Stange, G., Biber, J., Murer, H. 1993. Expression cloning of human and rat renal cortex Na/Pi cotransport. *Proc. Natl. Acad. Sci. USA* **90:**5979–5983
12. Markovich, D., Forgo, J., Stange, G., Biber, J., Murer, H. 1993. Expression cloning of rat renal Na/SO_4 cotransport. *Proc. Natl. Acad. Sci. USA* **90:**8073–8077
13. Markovich, D., Bissig, M., Sorribas, V., Hagenbuch, B., Meier, P.J., Murer, H. 1994. Expression of rat renal sulfate transport systems in *Xenopus laevis* oocytes. *J. Biol. Chem.* **269:**3022–3026
14. McLatchie, L., Fraser, N.J., Main, M.J., Wise, A., Brown, J., Thompson, N., Solari, R., Lee, M.G., Foord, S.M. 1998. RAMPs regulate the transport and ligand specificity of the calcitonin-receptor-like receptor. *Nature* **393:**333–339
15. Mendelssohn, D.C., Silverman, M. 1989. A D-mannose transport system in renal brush-border membranes. *Am. J. Physiol.* **257:** F1100–F1107
16. Murer, H., Gmaj, P. 1986. Transport studies in plasma membrane vesicles isolated from renal cortex. *Kidney Int.* **30:**171–186
17. Panneerselvam, K., Freeze, H.H. 1996. Mannose enters mammalian cells using a specific transporter that is insensitive to glucose. *J. Biol. Chem.* **271:**9417–9421
18. Pitkänken, E., Pitkänen, O.M. 1992. Renal tubular reabsorption of 1,5-anhydro-D-glucitol and D-mannose in vivo in the rat. *Pfluegers Arch.* **420:**367–375
19. Pritchard, J.B., Booz, G.W., Kleinzeller, A. 1982. Renal sugar transport in the winter flounder VI. Reabsorption of D-mannose. *Am. J. Physiol.* **242:**F415–422
20. Reinhardt, J., Veyhl, M., Wagner, K., Gambaryan, S., Dekel, C., Akhoundova, A., Korn, T., Koepsell, H. 1999. Cloning and characterization of the transport modifier RS1 from rabbit which was previously assumed to be specific for Na^+-D-glucose cotransport. *Biochim. Biophys. Acta* **1417:**131–143
21. Saint-Pol, A., Codogno, P., Moore, S.E. 1999. Cytosol-to-lysosome transport of free polymannose-type oligosaccharides. Kinetic and specificity studies using rat liver lysosomes. *J. Biol. Chem.* **274:**13547–13555
22. Silverman, M., Aganon, M.A., Chinard, F.P. 1970. Specificity of monosaccharide transport in dog kidney. *Am. J. Physiol.* **218:**743–750
23. Silverman, M., Ho, L. 1993. Kinetic characterization of Na^+/D-mannose cotransport in dog kideny: comparison with Na^+/D-glucose cotransport. *Biochim. Biophys. Acta* **1153:**34–42
24. Sorribas, V., Markovich, D., Werner, A., Biber, J., Murer, H. 1993. Expression of Na/Pi cotransport from opossum kidney cells in *Xenopus laevis* oocytes. *Biochim. Biophys. Acta* **1178:**141–145
25. Sorribas, V., Markovich, D., Hayes, G., Stange, G., Forgo, J., Biber, J., Murer, H. 1994. Cloning of a Na/Pi cotransporter from opossum kidney cells. *J. Biol. Chem.* **269:**6615–6621
26. Sorribas, V., Lötscher, M., Loffing, J., Biber, J., Kaissling, B., Murer, H., Levi, M. 1996. Cellular mechanisms of the age-related decrease in renal phosphate reabsorption. *Kidney Int.* **50:**855–863
27. Soyama, K. 1984. Enzymatic determination of D-mannose in serum. *Clin. Chem.* **30:**293–294
28. Thorens, B. 1993. Facilitated glucose transporters in epithelial cells. *Annu. Rev. Physiol.* **55:**591–608
29. Turk, E., Wright, E.M. 1997. Membrane topology motifs in the SGLT cotransporter family. *J. Membrane Biol.* **159:**1–20
30. Veyhl, M., Spangenberg, J., Puschel, B., Poppe, R., Dekel, C., Fritzsch, G., Haase, W., Koepsell, H. 1993. Cloning of a membrane-associated protein which modifies activity and properties of the Na(+)-D-glucose cotransporter. *J. Biol. Chem.* **268:**25041–25053
31. Werner, A., Moore, M.L., Mantei, N., Biber, J., Semenza, G., Murer, H. 1991. Cloning and expression of cDNA for a Na/Pi cotransport system of kidney cortex. *Proc. Natl. Acad. Sci. USA* **88:**9608–9612
32. Yamanouchi, T., Shinohara, T., Ogata, N., Tachibana, Y., Akaoka, I., Miyashita, H. 1993. Common reabsorption system of 1,5-ahydro-D-glucitol, fructose, and mannose in rat renal tubule. *Biochim. Biophys. Acta* **1291:**89–95